Published in final edited form as:
*Epilepsia*. 2009 April ; 50(4): 664–677. doi:10.1111/j.1528-1167.2008.01989.x.

# Blood–brain barrier damage and brain penetration of antiepileptic drugs: Role of serum proteins and brain edema

**Nicola Marchi**[*,†,‡], **Giulia Betto**[*,†,‡], **Vincent Fazio**[*,†,‡], **Quinyuan Fan**[*,†,‡], **Chaitali Ghosh**[*,†,‡], **Andre Machado**[§], and **Damir Janigro**[*,†,‡,¶]

[*] Department of Neurological Surgery, Cleveland Clinic Foundation, Cleveland, Ohio, U.S.A

[†] Department of Cell Biology, Cleveland Clinic Foundation, Cleveland, Ohio, U.S.A

[‡] Department of Cerebrovascular Research, Cleveland Clinic Foundation, Cleveland, Ohio, U.S.A

[§] Center for Restorative Neuroscience, Cleveland Clinic Foundation, Cleveland, Ohio, U.S.A

[¶] Department of Molecular Medicine, Cleveland Clinic Foundation, Cleveland, Ohio, U.S.A

## SUMMARY

**Purpose:** Increased blood–brain barrier (BBB) permeability is radiologically detectable in regions affected by drug-resistant epileptogenic lesions. Brain penetration of antiepileptic drugs (AEDs) may be affected by BBB damage. We studied the effects of BBB damage on brain distribution of hydrophilic [deoxy-glucose (DOG) and sucrose] and lipophilic (phenytoin and diazepam) molecules. We tested the hypothesis that lipophilic and hydrophilic drug distribution is differentially affected by BBB damage.

**Methods:** In vivo BBB disruption (BBBD) was performed in rats by intracarotid injection of hyperosmotic mannitol. Drugs (H3-sucrose, 3H-deoxy-glucose, 14C-phenytoin, and C14-diazepam) or unlabeled phenytoin was measured and correlated to brain water content and protein extravasation. In vitro hippocampal slices were exposed to different osmolarities; drug penetration and water content were assessed by analytic and densitometric methods, respectively.

**Results:** BBBD resulted in extravasation of serum protein and radiolabeled drugs, but was associated with no significant change in brain water. Large shifts in water content in brain slices in vitro caused a small effect on drug penetration. In both cases, total drug permeability increase was greater for lipophilic than hydrophilic compounds. BBBD reduced the amount of free phenytoin in the brain.

**Discussion:** After BBBD, drug binding to protein is the main controller of total brain drug accumulation. Osmotic BBBD increased serum protein extravasation and reduced free phenytoin brain levels. These results underlie the importance of brain environment and BBB integrity in determining drug distribution to the brain. If confirmed in drug-resistant models, these mechanisms could contribute to drug brain distribution in refractory epilepsies.

### Keywords

Phenytoin; MRI; Multiple drug resistance; Drug delivery; Drug design; Pharmacokinetics

Address correspondence to Damir Janigro, Ph.D., Director of Cerebrovascular Research, Professor of Molecular Medicine, Cleveland Clinic Foundation, NB-20 LRI 9500 Euclid Ave, Cleveland, OH 44195, U.S.A. janigrd@ccf.org.

We read the Journal's position on issues involved in ethical publication and confirm that this report is consistent with those guidelines. None of the authors has any conflict of interest to disclose.

The blood–brain barrier (BBB) protects the brain from harmful substances in the bloodstream, while supplying the brain with the nutrients required for proper function. The endothelial cell cerebrovasculature lining also regulates brain penetration of drugs. Because of the presence of such complex and yet delicate mechanisms of vascular protection, pharmacologic targeting of central nervous system (CNS) pathologies was and remains a challenge. In general, it is assumed that breaching the BBB will improve CNS drug delivery (Kroll & Neuwelt, 1998), but altered BBB function associated with CNS pathologies such as epilepsy is also a characteristic of pharmacokinetic drug resistance (Oby & Janigro, 2006). Therefore, the interplay between BBB function or failure, and drug delivery is more complex than originally believed.

Is there a link between leakage of the BBB, seizure-epileptic pathology, and multiple drug resistance? Several evidences have shown BBB damage and profound remodeling of the cerebrovasculature during or immediately after seizures (Marchi et al., 2006, 2007b). This has been interpreted as a vascular consequence of spontaneous seizures. It has also been repeatedly shown that BBB leakage is sufficient to promote seizures (Oby & Janigro, 2006; Marchi et al., 2007a,b; Uva et al., 2007) or epileptogenesis (Seiffert et al., 2004; van Vliet et al., 2007). Whatever the temporal or causal relationship between BBB leakage and seizures, it is clear that the epileptic brain is characterized by an abnormal blood–brain interface.

The integrity of the BBB is clinically evaluated with magnetic resonance imaging (MRI) techniques. Although $T_1$-contrast enhancement ($Gd^{++}$) is a reliable imaging method for direct testing of BBB permeability, structural changes at a cellular level and changes of the distribution of water between the extra- and intracellular compartments can be assessed by diffusion-weighted imaging (DWI) and by calculating the extent of passive water motion or diffusivity (apparent diffusion coefficient, ADC). Periictal and postictal human studies using DWI or diffusion tensor imaging (DTI) showed, in some cases, transiently decreased local diffusivity, potentially in concordance with the epileptic zone (Vincent et al., 1995; Flink & Atchison, 2003; Lang & Vincent, 2003; Vernino, 2007). Diffusion studies have also demonstrated areas of significantly increased diffusivity in patients with partial epilepsies during the interictal period (Diehl et al., 1999, 2001; Hufnagel et al., 2003; Diehl et al., 2005). These results suggest that abnormal cerebrovascular and parenchymal homeostatic mechanisms are altered in epileptics.

In human epilepsy, overexpression of drug-resistance efflux proteins at the BBB has been studied extensively in the framework of antiepileptic drug (AED) refractoriness, but additional mechanisms have also been proposed (Loscher & Potschka, 2005; Oby & Janigro, 2006). Given that the pathology of drug-resistant epilepsy often reveals morphologic and functional abnormalities of the BBB, protein extravasation, and brain edema, it is reasonable to hypothesize that the physical–chemical properties of AEDs will differently predict CNS drug delivery to the epileptic focus. For example, most AEDs are highly lipid soluble and tightly protein bound, and their permeability across an intact BBB is controlled by parameters. It is possible that altered brain water content or protein extravasation combined with overexpression of drug transporters may affect the distribution of AEDs.

We have focused our study on the consequences of BBB damage on serum protein extravasation and brain water content. Because this was induced acutely and by iatrogenic means, the results may bear specific relevance for sudden episodes of BBB disruption (BBBD), as seen in traumatic brain injury (Schmidt & Grady, 1993; Korn et al., 2005; Tomkins et al., 2008). For this pilot study we used the hydrophilic radiolabel compounds $^{3}$H-deoxy-glucose (DOG) and $^{3}$H-sucrose (SUC) and the lipophilic AEDs $^{14}$C-phenytoin (PHT) and $^{14}$C-diazepam (DIA).

# Methods

## Animals and tissue sample preparation

Rats were housed in a controlled environment (21 ± 1°C; humidity 60%; lights on 08:00 a.m.–8:00 p.m.; food and water available ad libitum). Procedures involving animals and their care were conducted in conformity with the institutional guidelines that are in compliance with international laws and policies. A total of 50 rats (Sprague-Dawley, male, 200–250 g) were used. In particular: 10 rats for in vitro drug uptake experiments (n = 5 slices/ condition, a total of 30 slices was used for experiments shown in Fig. 4D), 5 rats for determination of water content in in vitro slices (n = 5 slices/condition, total of 15 was used for Fig. 4C), 20 rats for BBBD and radiolabeled drug brain uptake (n = 5 rats each experimental group, see Fig. 3), 5 rats for the histologic evaluation of the BBBD in vivo (see Figs. 1 and 2), 5 for the determination of water content in vivo after BBBD (see Fig. 4A), and 5 for high performance liquid chromatography (HPLC) analysis (see Fig. 4B, C). All rats were anesthetized [xylazine (20 mg/ml): ketamine (100 mg/ml), ratio 1:9, dose 1 $\mu$l/g] prior to surgical procedures. Blood was withdrawn from the right heart ventricle; brain areas (coordinate from Paxinos and Watson, approximately: frontal cortex 6.7–1.7 mm, parietal cortex 1.7 to −4.6, temporal lobe −4.6 to cerebellum) were resected and processed for radioactivity evaluation. Serum was obtained after centrifugation at 1,500***g*** for 10 min at 4°C.

## Intracarotid injection of hyperosmolar mannitol

After anesthesia, a 2–3 cm vertical incision was made from the suprasternal notch to below the chin. After exposure of the sternothyroid muscle, the common carotid artery was exposed and was separated from the posteriorly placed vagal nerve. After exposure of the bifurcation of internal and external carotid arteries, a silk tie (3-0, Ethicon, 24″, Ethicon, Sommersville, NJ, U.S.A.) was looped around the external branch of the external carotid artery (ECA), while a micro-clamp was positioned ready at the common carotid artery (CCA). In temporal sequences the following steps were then performed within 2–3 min: (1) clamp the CCA; (2) ligate the distal ECA, leaving approximately 5 mm stump proximally; (3) insert the polyethylene catheter (27 gauge) into the proximal stump of the ECA toward the bifurcation; (4) tighten the silk tie around the catheter; (5) injection of a hyperosmolar mannitol solution (1.4 M bolus in saline, 0.1 ml/s, 2 ml); (6) remove the catheter and ligate the proximal stump of the ECA; and (7) release the clamp at the CCA. Sham procedures were conducted using identical protocol and injecting 2 ml of sterile phosphate-buffered saline (PBS) instead of the mannitol hyperosmolar solution.

## In vitro hippocampal slices

Rats were deeply anesthetized with isoflurane and then decapitated. The brain was quickly removed from the skull and immediately placed into ice-cold oxygenated cutting solution (95% $O_2$; 5% $CO_2$), composed in mM of 2.5 KCl, 28 $NaHCO_3$, 1.25 $NaHPO_4$, 7 dextrose, 7 $MgCl_2$, 0.5 $CaCl_2$, 235 sucrose, 1 ascorbic acid, 3 Na-pyruvate. Brains were subsequently cut in the coronal plane into slices of 450-$\mu$m thickness using a Vibratome 3000 (The Vibratome Co., St. Louis, MO, U.S.A.). Slices were kept at room temperature and pH 7.4 in a chamber containing oxygenated artificial cerebrospinal fluid (ACSF) of the composition (in mM): 120 NaCl, 3.1 KCl, 3 $MgCl_2$, 26 $NaHCO_3$, 1.25 $KH_2PO_4$, 10 dextrose, 1 $CaCl_2$, 1 ascorbic acid, 3 Na-pyruvate. After 1 h in recovery, the slices were transferred to a chambers containing ACSF of different osmolarity (from 250–390 mOsm) and incubated for 30 min before exposure to the drugs. Changes in osmolarity were achieved by adding or removing the appropriate amounts of mannitol to the ACSF while keeping the ionic concentrations constant. The isoosmolar solution (356 mOsm) consisted of (in mM): 60 NaCl, 60 mannitol, 3.1 KCl, 2 $MgCl_2$, 26 $NaHCO_3$, 1.25 $KH_2PO_4$, 10 dextrose, 2 $CaCl_2$.

### Radiolabeled chemical injection and quantification

$H^3$-sucrose, $^3H$-deoxy-glucose, $^{14}C$-phenytoin, and $C^{14}$-diazepam (1 $\mu$Cu, Sigma-Aldrich, St. Louis, MO, U.S.A., specific activity $^3H$: 20 and 12 Cu/mmol; $^{14}C$: 53.1 and 56 mCu/mmol, respectively) dissolved in 500 $\mu$l of saline were injected after sham procedures (with isoosmolar PBS) or after BBBD through the intracarotid catheter. After 3 min, peripheral blood was drawn from the left heart ventricle and brains were dissected out (frontal, parietal, occipital cortex, and cerebellum). Radioactivity was determined by a $\beta$-counter (Beckman-Coulter, Fullerton, CA, U.S.A.). Brain samples were weighed and homogenized with ice-cold solubilizing buffer [10 mM Tris-HCl, pH 7.4, 1 mM ethylene diamine tetraacetic acid (EDTA), 150 mM sodium chloride, 60 mM octylglycoside] using a glass potter (150 $\mu$l of solution per 10 mg of tissue). Radioactivity in brain was normalized by tissue weight. Radioactivity counted in serum was normalized by volume. Brain-to-plasma ratios for each drug were then calculated from these values.

### Evans Blue injection for BBBD assessment

Dye solutions [Evans Blue, 0.2% in buffered saline (10 ml), Sigma-Aldrich or fluorescein isothiocyanate (FITC)–labeled albumin] were slowly injected in the left ventricle at a rate of 1 ml/min as described previously (Cavaglia et al., 2001). Three minutes after injection, rats were killed by decapitation and their brains immersion-fixed for 48 h in 4% paraformaldehyde pH 7.4, and then cryoprotected overnight in a 20% sucrose solution, frozen in isopentane (−60° C), and stored at −80°C. Coronal sections (40 $\mu$m) were cut on a cryostat throughout the septo-temporal extension of the hippocampus and collected in 0.05 M PBS. Sections were then washed with saline and mounted in a Mowiol-based mounting medium containing 0.1% para-phenylenediamine hydrochloride and DAPI staining for nuclei. Fluorescent-stained sections were examined using a Leica confocal laser-scanning microscope.

### FITC-Albumin and fluorescent doxorubicin injection

A solution containing 10 mg/ml of FITC-albumin and red fluorescent doxorubicin (1 $\mu$M) was injected as described earlier. Doxorubicin is used as a small red fluorescent tracer (540 Da).

### Percent water measurement of brain tissue or brain slices

**Preparation and use of the gradient column—**Kerosene and bromobenzene were mixed as follows: Solution A, specific gravity (SG) of 0.950: 27.0% bromobenzene (SG = 1.48413) and 73.0% kerosene (SG = 0.75183); Solution B, SG = 1.0700: 43.4% bromobenzene and 56.6% kerosene. The denser mixture (1.0700) was placed in a 250-ml graduated cylinder first and the lighter liquid (0.9500) carefully layered above it using a sterilized, glass pipette. The gradient is prepared by mixing the solutions with a soft copper wire coiled at one end. Standardization of the gradient is always done just prior to measuring SG of a series of samples. Standards are prepared with $K_2SO_4$ dried overnight at 100° C. The SG standards generally used and the grams (per liter) of $K_2SO_4$ needed to prepare them are as follows: 1.0200 (24.7), 1.0300 (37.0), 1.0400 (49.2), 1.0500 (61.3), and 1.0600 (73.3). Duplicate volumes (5–10 $\mu$l) of each standard are placed in the column, and a standard curve is prepared from their position in the gradient mixture. A standard or sample is added to the column and its position is determined 1–2 min later using the graduated scale on the cylinder. The percent water calculation is made based on a series of tissue samples in which edema or dehydration are accomplished using a hyper-or hypoosmotic solution. The percent dry weight is calculated by measuring the wet weight of the tissue prior to treatment and subtracting from it the dry weight of the sample (after drying overnight at 100° C) divided by the same wet weight. A linear correlation is plotted of % Water versus Specific Gravity (SG), and from the formula of this line percent water is calculated from the measured SG in subsequent experiments. See for details Marmarou et al. (1978).

### Estimation of free and total phenytoin by HPLC-UV

Phenytoin (free and total) extravasation through BBB and BBBD was estimated by HPLC UV detection (Agilent 1100 Series) system (Patil & Bodhankar, 2005). Chromatographic separations were performed using a Zorbax Eclipse Plus C18 stainless steel column (4.6 × 150 mm, 3.5 $\mu$m), supplied by Agilent Technologies, Santa Clara, CA, U.S.A. Phenytoin (PHT) was purchased from Sigma-Aldrich. Solvents used were of HPLC grade purchased from Fisher Scientific, Pittsburgh, PA, U.S.A., and all other chemical and reagents were of analytical grade. Preparation of standard solutions: A stock solution containing 1 mg/ml of PHT was prepared in methanol. The calibration standards (0.5, 1, 5, 10, 20, and 40 $\mu$g/ml) were prepared by further dilution of stock solution with drug-free rat plasma. The standards with drug-free rat plasma were filtered through 0.2-$\mu$m membrane filter. All solutions were stored at −20°C. Chromatographic conditions: The mobile phase consisted of phosphate buffer (10 mM)-methanol-acetonitrile-acetone (55:22:12:11, v/v/v/v) at pH adjusted to 7.0 with 0.5 M NaOH. The mobile phase was always freshly prepared and was degassed and filtered by using a Millipore (Bedford, MA, U.S.A.) vacuum filter system equipped with 0.45-$\mu$m membrane filter. The 10-mM phosphate buffer was prepared by dissolving 1.36 g of potassium dihydrogen phosphate ($KH_2PO4$) in 1 L of doubly distilled water. Chromatography was performed at ambient temperature by pumping the mobile phase at a flow rate of 1.2 ml/min. The column effluent was monitored at 210 nm. Extraction procedure: Rat brain regions of interest were homogenized in methanol/water (60/40, v/v; 10 mg tissue/100 $\mu$l). For free drug assessment, 100 $\mu$l of tissue or plasma sample taken and 0.2 M perchloric acid added, vortex for 30 s, and for total drug 100 $\mu$l of sample was directly taken, and both free and total drug samples were centrifuged at 4,900***g*** for 10 min. The supernatant was filtered through 0.2-$\mu$m membrane filter, and 20 $\mu$l of filtrate was injected onto the column. Specificity and precision: The method was evaluated for specificity by analyzing different batches of drug-free rat serum to check the interference of peaks of endogenous components of serum. The different batches of serum were found to be free from interfering components at the retention time of phenytoin. The intraday precision was determined from replicate analysis and covering different concentration of the calibration curve. Stability: Phenytoin is stable in serum/plasma when stored at −20°C for at least 4 weeks. The extracted drug samples were stored at room temperature (25°C) for 24 h prior to analysis.

### Statistical analysis

Data are expressed as means ± SEM. For parametric variables (e.g., brain or serum drug levels), differences between populations were assessed by analysis of variance (ANOVA) (significance $p < 0.05$). Bonferroni analysis was used to account for comparisons of multiple parameters among groups. JMP statistical software (v. 7.0, http://www.jmp.com) was used for analysis and data comparison.

## Results

### Osmotic opening of the BBB with intraarterial mannitol

The timing and intervals of the BBBD procedure used for the experiments are shown in Fig. 1A. Following osmotic BBBD, gross anatomic examination showed superficial and parenchymal Evans Blue staining (Fig. 1B), whereas detailed fluorescent microscopy evaluation revealed discrete clouds of dye extravasation (Fig. 1C, D). We evaluated the extent of BBB opening in frontoparietal brain sections (Fig. 1C), in temporal cortex (Fig. 1D), and in the cerebellum. Evans Blue extravasation was present in all the cerebral sections analyzed by fluorescent microscopy. Cerebellar BBBD was minimal compared to the anterior brain, as expected following injection of mannitol solution through the internal carotid artery (not shown). No consistent BBB leakage was observed in the contralateral hemisphere. Note that because Evans Blue binds irreversibly and avidly to plasma protein (Table 1), intravenously

injected Evans Blue binds irreversibly to serum albumin, and its distribution reflects albumin exchange between the intravascular and extravascular tissue compartments(Wolman et al., 1981).

## Evaluation of drug-to-plasma distribution after BBBD

After osmotic opening of the BBB, we first assessed the pattern of drug penetration using radiolabeled compounds. Use of radiolabeled compounds reflects measurements of total drug uptake in brain and does not allow discriminating free from protein bound drugs. We used two combinations of hydrophilic and lipophilic molecules ($^{3}$H-deoxy-glucose (DOG) + $^{14}$C-diazepam or $^{3}$H-sucrose + $^{14}$C-phenytoin). The experimental procedure is indicated in Fig. 1A. Two to three minutes after BBBD, the cocktails of drugs was injected through the carotid artery. Rats were sacrificed 2–3 min later. Brain radiotracer levels, measured in both hemispheres, were normalized to serum levels after injection. Sham procedures were performed by injecting a bolus of saline into the internal carotid artery. We analyzed the brain-to-plasma ratio in the brain areas used to quantify protein extravasation in Fig. 1. No difference in brain drug uptake was measured when comparing nondisrupted hemispheres (i.e., contralateral to BBBD or after sham BBBD with saline, Fig. 2A).

As expected, the brain-to-plasma ratio for the lipophilic $^{14}$C-diazepam was greater compared to the hydrophilic $^{3}$H-deoxy-glucose (DOG). Such a trend was identical in the two hemispheres analyzed and for all the brain regions evaluated. These results show that the surgical procedure itself does not damage the cerebrovasculature (e.g., Fig. 2A). Identical findings were obtained with $^{14}$C-phenytoin and $^{3}$H-sucrose: The drugs distributed comparably in both hemispheres and accumulated in the CNS following their octanol/water partition coefficient, thereby confirming the integrity of the BBB after the sham procedures.

After BBBD, a remarkable increase in radiolabeled drug brain uptake was measured in the treated hemisphere compared to the contralateral side (Fig. 2B, C). In the hemisphere affected by the osmotic BBB opening procedure, brain uptake was dramatically increased for lipophilic drugs ($^{14}$C-diazepam, 45-fold; $^{14}$C-phenytoin, 30-fold) and to a lesser extent ($^{3}$H-DOG, 10-fold; $^{3}$H-SUC, 8-fold) for their hydrophilic counterparts. These data show that BBBD dramatically increases lipophilic but not hydrophilic radiolabeled drug uptake.

## Influence of octanol/water partition and CNS water content on drug-to-plasma ratio after BBBD

When the results of these in vivo experiments are plotted against the effect of oil-to-water partition coefficient (log P, Davson & Segal, 1996) of the tracers used, it becomes apparent that although drug distribution follows the expected behavior in nondisrupted hemispheres, this is dramatically exaggerated after BBBD (Fig. 2). However, we also wished to consider the influence of water redistribution on drug permeation after BBBD. This was dictated by the hypothesis that lipophilic, water insoluble drugs will partition differently after BBBD compared to their water soluble hydrophilic counterparts. Specific gravity and water content were measured by densitometric assay in both hemispheres 3 min after BBBD (Fig. 3A). In parallel experiments, drug diffusion in brain slices exposed to osmotic manipulations was also determined (Fig. 3C, D). Comparison of brain penetration in vivo and in vitro was performed to fully assess the relevance of individual components (BBB, protein extravasation and drug binding, and water content) on drug distribution.

As expected based on previous findings by others (Rapoport et al., 1980; Ziylan et al., 1984), the brain water content was only insignificantly affected by the BBBD procedure, at least within the time frame of our studies. Only slight differences in percent water content following BBBD were measured in vivo (81.4% BBBD vs. 81.8% contralateral, $p = 0.07$). Fig. 3 shows the

brain-to-plasma distribution (y-axis) of the drugs used in relation to respective octanol/water partition coefficients (x-axis) and water content (z-axis). Data points on the y-axes are calculated from the mean of the drug levels showed in Fig. 2 (frontal cortex, parietal cortex, and temporal lobe). Standard error (SE) is indicated next to each point of BBBD. SE for contralateral and in vitro experiments is not displayed, since it was less than ± 10% of each value indicated. The percentage of drug bound to plasma is also shown as a label in *blue*. Therefore, although the water shift measured after BBBD appeared to be too marginal to affect drug distribution across the BBB, a large difference in drug uptake between disrupted and nondisrupted hemispheres was seen. To further study the effect of water on drug uptake, we tested the effects of a much larger shift in water content achieved by osmotic manipulation of brain slices in vitro. Slices were perfused with radiolabeled tracers to mimic the in vivo experiment but in absence of a BBB or serum protein. The shift in water content in slices led to modest effects on drug distribution compared to in vivo (note that the different y-axes in Fig. 3B, D) despite a much larger shift in water content. These results suggested that water content in brain plays a small effect on drug partition in the CNS, but failed to explain why BBBD has such a pronounced effect of lipophilic drug uptake (shown in Figs, 2B, C and 3B).

## FITC-Albumin and drug extravasation

BBB function and the effects of disruption on drug permeability were further studied by intravascular perfusion with fluorescently labeled serum protein (FITC-albumin) and red fluorescent doxorubicin (Fig. 4A). Although Evans Blue is bound to virtually all serum proteins, FITC-albumin is a tracer of the most common serum protein. Drug and labeled protein perfusion was performed in a fashion identical to that used for experiments with radiolabeled tracers, but fluorescent doxorubicin was used at therapeutically relevant concentrations (1 $\mu$M). In the presence of an intact BBB, both markers were confined intravascularly because of the low permeability of serum proteins and the tight binding of doxorubicin to albumin (Table 1). After BBBD, extravasation of fluorescent albumin was temporally and topographically identical to doxorubicin leakage. These data suggested that protein extravasation may increase the total drug amount in the CNS, as also shown in Fig. 2 with radiotracers.

The amount of free drug could not be fully appreciated with radioactive or fluorescent techniques, so we also measured the extravasation of free and total phenytoin under conditions of osmotic BBBD or in presence of an intact BBB (Fig. 4B). Note that the levels of free phenytoin were greatly decreased after complete BBBD, whereas the total drug measured was drastically increased (see panel C). After analyzing data from four attempts to induce a BBBD, we noticed that the extent of drug bound to protein varied from experiment to experiment. This is because mannitol does not always produce full disruption of the BBB. We thus plotted the extent of disruption against the percentage of free drug in the brain. These data (Fig. 4C) encompass a broad range of levels of BBBD enabling exponential fitting of BBBD versus percent of drug according to the equation shown. Note that (*insert*) there was a linear relationship between decreased free drug levels and BBBD ($p < 0.01$, $r = 0.92$). When all data points were fitted, an exponential relationship was seen, with asymptotic behavior at levels of disruption identical to those mimicking the conditions under which the results in Fig. 4B were obtained. In the *left panel* of Fig. 4D, the level of drug measured by HPLC under conditions of intact BBB in serum and brain is plotted against time (in minutes). In the *right panel*, the same are plotted but measurements were taken after BBBD. Drug levels are reported as area under the curve (AUC) measured in HPLC graphic output. Note that free serum and free brain levels coincided in the latter because of the shift of protein bound–unbound drug into the brain.

## Discussion

Our data shed light on the importance of brain environment and BBB integrity in determining drug distribution to the brain. We found that: (1) drug lipophilicity (log P) is a good predictor of drug penetration into the brain but that in the presence of BBBD the level of drug binding to protein is the main controller of total drug accumulation; (2) in vivo, acute BBBD did not affect parenchymal water content but caused serum protein extravasation into the brain; (3) in our experimental paradigm, water content did not appear to be the pivotal player controlling drug permeation; (4) regions of impaired BBB function are characterized by lower levels of free drug (phenytoin) compared to regions of intact cerebrovasculature.

In normal brain, several mechanisms regulate, directly or indirectly, brain penetration of drugs to their site of action. These include metabolic transformation by specialized enzymes, which determine the plasma levels of drug (Meyer & Zanger, 1997; Meyer et al., 2007), binding of drugs to serum protein (Zhou et al., 2005), drug transporters at the BBB (Abbott et al., 2001; Oby & Janigro, 2006; Oby et al., 2006; Sisodiya et al., 2006), and transformation of “pro-drugs” into an active form. Interestingly, a conformational change in the albumin molecule takes place during its trans-BBB passage, which results in enhanced capillary dissociation of protein-bound ligands in the capillary milieu. This mechanism required an intact and functional BBB. In conditions in which the BBB is damaged, this mechanism could be lost, therefore, contributing to the extravasation of protein-bound drug (Cornford et al., 1983).

### BBB leakage, protein extravasation, and epilepsy

An important question relates to the relevance of iatrogenic, hyperosmolar BBB disruption to the leakage of the BBB observed in seizure disorders. In the presented study, we tested our hypothesis with an experimental paradigm associated with a diffuse damage of the BBB, therefore, constituting a proof-of-principle approach to study the effect that BBB damage could have on serum protein extravasation, brain edema formation, and drug brain penetration. In our study we did not use animals that were epileptic and resistant to AEDs.

Several pieces of evidence point to BBB damage during or immediately after seizures. A profound remodeling of the cerebrovasculature also associated with leakage and extravasation of serum proteins is observed in rodent models of temporal lobe epilepsy and has been attributed to spontaneous seizures (Fabene et al., 2003; Marchi et al., 2007b; Uva et al., 2007). Extravasation of serum albumin was demonstrated in temporal lobe epilepsy (Cornford et al., 1998). Conversely, it has also been repeatedly shown that BBB leakage promotes seizures (Oby & Janigro, 2006; Marchi et al., 2007a, 2007b; Uva et al., 2007) or epileptogenesis (Seiffert et al., 2004; van Vliet et al., 2007). Whatever the temporal relationship between BBB leakage and seizures, it is clear that epileptic brain is characterized by an abnormal blood–brain interface. In these reports the integrity of the BBB was mechanically disturbed using different experimental paradigms, which are, however, based on the induction of an osmotic shock. Interestingly, BBB permeability can also be enhanced because of altered transendothelial transport mechanisms. For instance, an increased number of pinocytotic vesicles at the BBB was observed in kindled animals with cortical dysplasia as induced by irradiation (Kaya et al., 2008).

### Brain edema in epileptic brain and after BBBD

It has been long suspected that seizures may induce cell edema. Routine MR techniques allow the detection of focal cortical and hippocampal swelling after prolonged seizures in the area of the seizure focus (Sammaritano et al., 1985). $T_2$ imaging often shows focal increased signal intensity (Scott et al., 2002). The signal increase may involve cortical or limbic structures, particularly the hippocampus, where postictal changes can be unilateral or bilateral

(Wieshmann et al., 1997; Sokol et al., 2003). Similar results are obtained with DWI, which usually overlaps with $T_2$-imaging findings. Both are suggestive of cytotoxic edema, resulting from metabolic mismatch between available energy and demand to clear extra- and intracellular ion accumulation resulting from excessive seizure activity. Whatever the changes in osmotic and solvent status in regions of disrupted BBB, it is significant that our results point against brain edema as a major determinant of drug partition in brain with a leaky BBB, or in absence of BBB (in vitro).

We wish to point out that *seizures*, not *epilepsy*, are common results of mannitol-induced BBBD. This original finding from our laboratory has recently been independently confirmed (Elkassabany et al., 2008), and a summary of the BBBD experience in a multicenter trial will be released shortly. We would also like to point out that iatrogenic mannitol as used for our experiments is not commonly employed, since its use is limited to treatment of selected brain tumors, primary central nervous system lymphoma (PCNSL) (Neuwelt et al., 1983). In contrast, therapeutic mannitol is commonly used for the treatment and prevention of brain herniation and in general to reduce or manage intracranial pressure. There are substantial differences between these two approaches, both in scope and in consequence. Iatrogenic mannitol is given intraarterially, under general anesthesia, and directly in the cerebrovasculature under radiologic guidance. The bolus injected has an osmolarity of 1.4 M. Therapeutic mannitol is usually given intravenously, and its osmolarity is around 390 mOsm. As to the link between epileptogenesis and BBBD, we acknowledge the work by VanVliet and colleagues (2007) in which a hypertonic solution of mannitol (although injected intravenously and not intracarotid as in our procedure) was used to enhance damage of the BBB in epileptic rats; these authors reported exacerbation of *epileptic* seizures. Finally, Seiffert and colleagues (2004) detected abnormal electroencephalographic activity after opening of the BBB obtained with cortical application of solution of bile salts, previously shown to open the tight junctions of brain capillaries.

### Mechanisms linking brain edema, BBBD, and protein extravasation in the brain

Our results have shown that acute BBBD does not cause a significant shift in water content, but others have shown edema at longer time intervals (Rapoport et al., 1980; Ziylan et al., 1984). When considering the formation of vasogenic edema, it is not clear why water may extravasate through a leaky BBB when total brain osmolarity is not substantially different from the osmolarity of serum (Davson & Segal, 1995). By pure diffusion motion, protein will escape across a leaky BBB from the blood into the brain according to their chemical gradients (see Results). However, it is unlikely that additional extravasation of other ionic solutes will drive sufficient water to account for brain swelling, since total ionic concentrations (and, therefore, osmolarity) in serum and brain are similar. Because vasogenic brain swelling is nevertheless commonly observed under conditions of impaired BBB function, and in particular in fluid attenuated inversion recovery (FLAIR) signals in epileptic brain, mechanisms other than different osmolarity between the two tissues may play an important additional role. In the case of epilepsy, it is well known that a significant shift of ions from the brain intracellular (neurons) to the extracellular compartment accompanies and follows seizures (Dietzel et al., 1989). For example, during seizures, extracellular potassium accumulation reaches levels that exceed 10-fold changes from baseline (Dietzel et al., 1989). This increased extracellular osmolarity may, therefore, drive more water from blood to brain, initiating a self-sustaining process leading to brain edema.

The early process of vasogenic edema formation may also *initiate* seizures. In nonepileptic brain but in the presence of a leaky barrier, protein extravasation occurs very early after BBBD as shown in Figs. 1 and 4A and in (Davson & Segal, 1995). For yet unknown reasons, albumin extravasation itself promotes proepileptogenic events (Seiffert et al., 2004). These events may

be sufficient to trigger seizures, followed by water influx into the brain driven by increased osmolarity of the extracellular space that occurs in seizures.

### AED protein binding

Many drugs are significantly bound to plasma proteins. Although this binding is not covalent and is often reversible, the drug–protein complex is too large to permeate across the BBB and, therefore, only the dissociated, "free" drug creates the gradient for concentration-driven accumulation into the brain (Stolp et al., 2005b). An important aspect of this is that the reservoir of total serum drug will provide free drug to the brain at a rate and with a gradient greater than that of the total drug. In fact, only the free drug (which is a fraction of the total) will partake in the trans-BBB gradient, resulting in free concentration of the drug that is higher than that measured in serum (see scheme in legend to Fig. 4). One of the earliest events following BBBD is the leakage of serum protein (Davson & Segal, 1995). When this occurs, it is reasonable to assume that both free and drug-bound protein will extravasate. This has been demonstrated by the fact that total drug levels after BBBD were increased several-fold in the disrupted hemisphere (e.g., Fig. 2) and was further confirmed by the fact that total CNS load of lipophilic drugs increased more than that of their water soluble counterparts. Therefore, after BBBD protein level in the CNS increases, so too does the fraction of bound drug that was previously acting as a serum reservoir. Under these conditions, the free brain drug will equate roughly to the levels in serum, owing to (1) loss of segregation from the reservoir and (2) diminished propensity to accumulate in the brain. This was demonstrated by measuring free drug (Fig. 4B, C) after BBBD.

### Methodologic considerations: Protein extravasation

To estimate protein extravasation, we employed two parallel approaches: fluorescently labeled albumin and Evans Blue bound to serum protein. There are significant differences between these two methods that need to be discussed (Wolman et al., 1981). In plasma, a considerable portion of fluorescein remains free and behaves like a non-proteic, small molecular weight barrier tracer. On the other hand, binding of the Evans Blue to albumin confers properties of a protein tracer. Our results failed to reveal significant differences, since the regions of interest were characterized by a similar extent of dye/fluorescence extravasation (data not shown). In addition, following extravasation of the tracers, the sodium fluorescein is relatively soon eliminated, whereas Evans Blue remains in the cellular elements of the brain parenchyma for a considerable time. This should not have affected our results, since only short time intervals were used to determine protein leakage.

### Methodologic considerations: Drug permeation

We intentionally used a variety of tracer techniques to determine how a breached BBB handles drug and protein diffusion. We took advantage of the availability of a fluorescently labeled small molecule to show that serum protein extravasation topographically coincided with doxorubicin extravasation after BBBD. This indirectly demonstrated that after BBBD an equilibration of serum protein with brain interstitial place occurs. To study how BBBD impacts AED levels in the CNS, we resorted to an alternative method. Total drug levels were measured by radiolabeled tracers, but to determine the ratio of free-to-bound AED we used HPLC analysis; both were performed in parallel to determination of brain water content and leakage of serum protein. Our results clearly show that BBBD decreased free phenytoin levels despite a large increase in total CNS drug levels.

### Significance for CNS drug delivery

Several clinical studies have suggested that breaching the BBB is beneficial for drug delivery (Kroll & Neuwelt, 1998). A study on lymphoma patients demonstrated a 5-fold increase of

methotrexate brain delivery after BBBD (Zylber-Katz et al., 2000). These findings are in agreement with our data on sucrose and deoxy-glucose, since methotrexate is a water-soluble drug (log P = −2.2) and with little tendency to bind to protein. Therefore, it appears that iatrogenic osmotic disruption of the BBB to deliver water-soluble drug to the brain is a sound approach, whereas use of lipophilic drugs to deliver to the edematous brain where protein extravasation occurred may be not equally effective. Increased risks of seizures during this procedure may be associated with such serum protein extravasation. Based on the studies presented here, this may be particularly important in the case of AEDs. An indirect proof that BBBD hinders drug delivery to the brain of lipophilic AED such as barbiturates is the fact that during osmotic opening of the BBB for the treatment of primary CNS, lymphoma seizures are often reported, despite profound anesthesia and prophylactic AED treatment (Marchi et al., 2007a; Elkassabany et al., 2008). Although patients might have been susceptible to seizures because of the presence of lymphoma, intraoperatively the extent of BBBD was the sole predictor of seizure occurrence. The relevance of the presence of brain lymphoma to seizures is discussed by the authors.

Our exploratory studies were by design limited by drug and animal model choices. The AEDs phenytoin and diazepam were chosen based on their high lipophilicity. As a comparison, we have used the hydrophilic compounds sucrose and deoxy-glucose. An obvious caveat of our study is that we did not use animals that were epileptic and refractory to drug treatment. The extent, timing, and means of BBBD (mannitol) differ from the BBB damage of epileptics.

In conclusion, our data suggest that brain parenchymal modifications (e.g., presence of serum protein and edema) consequent to damage of the BBB could affect drug brain penetration and distribution, possibly contributing to the phenomenon of pharmacologic refractoriness. Future experiments will clarify whether these concepts can be applied to chronic models of epilepsy and a broader choice of AEDs.

## Acknowledgments

Supported by NIH-NS43284, NIH-HL51614, NIH-NS46513, NIH-NS049514, and NIH-NS38195.

## References

Abbott, NJ.; Khan, EU.; Rollinson, C.; Reichel, A.; Janigro, D.; Dombrowski, S.; Dobbie, MBDJ. Drug resistance in epilepsy: the role of the blood-brain barrier. In: Ling, V., editor. Mechanisms of drug resistance in epilepsy: lessons from oncology. John Wiley; Chichester, UK: 2001. p. 38-47.

Cavaglia M, Dombrowski SM, Drazba J, Vasanji A, Bokesch PM, Janigro D. Regional variation in brain capillary density and vascular response to ischemia. Brain Res 2001;910:81–93. [PubMed: 11489257]

Cornford EM, Pardridge WM, Braun LD, Oldendorf WH. Increased blood-brain barrier transport of protein-bound anticonvulsant drugs in the newborn. J Cereb Blood Flow Metab 1983;3:280–286. [PubMed: 6874737]

Cornford EM, Hyman S, Cornford ME, Landaw EM, Delgado-Escueta AV. Interictal seizure resections show two configurations of endothelial Glut1 glucose transporter in the human blood-brain barrier. J Cereb Blood Flow Metab 1998;18:26–42. [PubMed: 9428303]

Davson, H.; Segal, MB., editors. Physiology of the CSF and blood-brain barriers. CRC Press; Boca Raton, FL: 1995. Breakdown of the barriers and cerebral edema; p. 525-572.

Davson, H.; Segal, MB., editors. Physiology of the CSF and blood-brain barriers. CRC; Boca Raton, FL: 1996. Blood-brain barrier; p. 49-91.

Dehouck B, Fenart L, Dehouck MP, Pierce A, Torpier G, Cecchelli R. A new function for the LDL receptor: transcytosis of LDL across the blood-brain barrier. J Cell Biol 1997;138:877–889. [PubMed: 9265653]

Diehl B, Najm I, Ruggieri P, Foldvary N, Mohamed A, Tkach J, Morris H, Barnett G, Fisher E, Duda J, Luders HO. Periictal diffusion-weighted imaging in a case of lesional epilepsy. Epilepsia 1999;40:1667–1671. [PubMed: 10565599]

Diehl B, Najm I, Ruggieri P, Tkach J, Mohamed A, Morris H, Wyllie E, Fisher E, Duda J, Lieber M, Bingaman W, Luders HO. Postictal diffusion-weighted imaging for the localization of focal epileptic areas in temporal lobe epilepsy. Epilepsia 2001;42:21–28. [PubMed: 11207781]

Diehl B, Symms MR, Boulby PA, Salmenpera T, Wheeler-Kingshott CA, Barker GJ, Duncan JS. Postictal diffusion tensor imaging. Epilepsy Res 2005;65:137–146. [PubMed: 16043327]

Dietzel I, Heinemann U, Lux HD. Relations between slow extracellular potential changes, glial potassium buffering, and electrolyte and cellular volume changes during neuronal hyperactivity in cat brain. Glia 1989;2:25–44. [PubMed: 2523337]

Elkassabany NM, Bhatia J, Deogaonkar A, Barnett GH, Lotto M, Maurtua M, Ebrahim Z, Schubert A, Ference S, Farag E. Peri-operative complications of blood brain barrier disruption under general anesthesia: a retrospective review. J Neurosurg Anesthesiol 2008;20:45–48. [PubMed: 18157025]

Fabene PF, Marzola P, Sbarbati A, Bentivoglio M. Magnetic resonance imaging of changes elicited by status epilepticus in the rat brain: diffusion-weighted and T2-weighted images, regional blood volume maps, and direct correlation with tissue and cell damage. Neuroimage 2003;18:375–389. [PubMed: 12595191]

Flink MT, Atchison WD. $Ca^{2+}$ channels as targets of neurological disease: Lambert-Eaton syndrome and other $Ca^{2+}$ channelopathies. J Bioenerg Biomembr 2003;35:697–718. [PubMed: 15000529]

Hufnagel A, Weber J, Marks S, Ludwig T, de Greiff A, Leonhardt G, Widmann G, Stolke D, Forsting M. Brain diffusion after single seizures. Epilepsia 2003;44:54–63. [PubMed: 12581230]

Kaya M, Gurses C, Kalayci R, Ekizoglu O, Ahishali B, Orhan N, Oku B, Arican N, Ustek D, Bilgic B, Elmas I, Kucuk M, Kemikler G. Morphological and functional changes of blood-brain barrier in kindled rats with cortical dysplasia. Brain Res 2008;1208:181–191. [PubMed: 18395195]

Korn A, Golan H, Melamed I, Pascual-Marqui R, Friedman A. Focal cortical dysfunction and blood-brain barrier disruption in patients with Postconcussion syndrome. J Clin Neurophysiol 2005;22:1–9. [PubMed: 15689708]

Kroll RA, Neuwelt EA. Outwitting the blood-brain barrier for therapeutic purposes: osmotic opening and other means. Neurosurgery 1998;42:1083–1099. [PubMed: 9588554]

Lang B, Vincent A. Autoantibodies to ion channels at the neuro-muscular junction. Autoimmun Rev 2003;2:94–100. [PubMed: 12848965]

Leveugle B, Ding W, Laurence F, Dehouck MP, Scanameo A, Cecchelli R, Fillit H. Heparin oligosaccharides that pass the blood-brain barrier inhibit beta-amyloid precursor protein secretion and heparin binding to beta-amyloid peptide. J Neurochem 1998;70:736–744. [PubMed: 9453569]

Loscher W, Potschka H. Drug resistance in brain diseases and the role of drug efflux transporters. Nat Rev Neurosci 2005;6:591–602. [PubMed: 16025095]

Marchi N, Guiso G, Caccia S, Rizzi M, Gagliardi B, Noe F, Ravizza T, Bassanini S, Chimenti S, Battaglia G, Vezzani A. Determinants of drug brain uptake in a rat model of seizure-associated malformations of cortical development. Neurobiol Dis 2006;24:429–442. [PubMed: 17027274]

Marchi N, Angelov L, Masaryk T, Fazio V, Granata T, Hernandez N, Hallene K, Diglaw T, Franic L, Najm I, Janigro D. Seizure-promoting effect of blood-brain barrier disruption. Epilepsia 2007a; 48:732–742. [PubMed: 17319915]

Marchi N, Oby E, Fernandez N, Uva L, de Curtis M, Batra A, Santaguida S, Barnes V, van Boxel A, Najm I, Janigro D. *In vivo* and *in vitro* effects of pilocarpine: relevance to epileptogenesis. Epilepsia 2007b;48:1934–1946. [PubMed: 17645533]

Marmarou A, Poll W, Shulman K, Bhagavan H. A simple gravimetric technique for measurement of cerebral edema. J Neurosurg 1978;49:530–537. [PubMed: 690681]

Meyer UA, Zanger UM. Molecular mechanisms of genetic polymorphisms of drug metabolism. Annu Rev Pharmacol Toxicol 1997;37:269–296. [PubMed: 9131254]

Meyer RP, Gehlhaus M, Knoth R, Volk B. Expression and function of cytochrome p450 in brain drug metabolism. Current Drug Metabolism 2007;8:297–306. [PubMed: 17504219]

Mielke JG, Murphy MP, Maritz J, Bengualid KM, Ivy GO. Chloroquine administration in mice increases beta-amyloid immunoreactivity and attenuates kainate-induced blood-brain barrier dysfunction. Neurosci Lett 1997;227:169–172. [PubMed: 9185677]

Neuberger TJ, Cornbrooks CJ, Kromer LF. Effects of delayed transplantation of cultured Schwann cells on axonal regeneration from central nervous system cholinergic neurons. J Comp Neurol 1992;315:16–33. [PubMed: 1541722]

Neuwelt EA, Balaban E, Diehl J, Hill S, Frenkel E. Successful treatment of primary central nervous system lymphomas with chemotherapy after osmotic blood-brain barrier opening. Neurosurgery 1983;12:662–671. [PubMed: 6410302]

Nishino H, Kumazaki M, Fukuda A, Fujimoto I, Shimano Y, Hida H, Sakurai T, Deshpande SB, Shimizu H, Morikawa S, Inubushi T. Acute 3-nitropropionic acid intoxication induces striatal astrocytic cell death and dysfunction of the blood-brain barrier: involvement of dopamine toxicity. Neurosci Res 1997;27:343–355. [PubMed: 9152047]

Oby E, Janigro D. The blood-brain barrier and epilepsy. Epilepsia 2006;47:1761–1774. [PubMed: 17116015]

Oby E, Caccia S, Vezzani A, Moeddel G, Hallene K, Guiso G, Said T, Bingaman W, Marchi N, Baumgartner C, Pirker S, Czech T, Lo RG, Janigro D. In vitro responsiveness of human-drug-resistant tissue to antiepileptic drugs: insights into the mechanisms of pharmaco-resistance. Brain Res 2006;1086:201–213. [PubMed: 16631625]

Patil KM, Bodhankar SL. Simultaneous determination of lamotrigine, phenobarbitone, carbamazepine and phenytoin in human serum by high-performance liquid chromatography. J Pharm Biomed Anal 2005;39:181–186. [PubMed: 15927430]

Rapoport SI, Fredericks WR, Ohno K, Pettigrew KD. Quantitative aspects of reversible osmotic opening of the blood-brain barrier. Am J Physiol 1980;238:R421–R431. [PubMed: 7377381]

Sammaritano M, Andermann F, Melanson D, Pappius HM, Camfield P, Aicardi J, Sherwin A. Prolonged focal cerebral edema associated with partial status epilepticus. Epilepsia 1985;26:334–339. [PubMed: 4006892]

Schmidt RH, Grady MS. Regional patterns of blood-brain barrier breakdown following central and lateral fluid percussion injury in rodents. J Neurotrauma 1993;10:415–430. [PubMed: 8145265]

Schubart DB, Rolink A, Schubart K, Matthias P. Cutting edge: lack of peripheral B cells and severe agammaglobulinemia in mice simultaneously lacking Bruton's tyrosine kinase and the B cell-specific transcriptional coactivator OBF-1. J Immunol 2000;164:18–22. [PubMed: 10604987]

Scott RC, Gadian DG, King MD, Chong WK, Cox TC, Neville BG, Connelly A. Magnetic resonance imaging findings within 5 days of status epilepticus in childhood. Brain 2002;125:1951–1959. [PubMed: 12183341]

Seiffert E, Dreier JP, Ivens S, Bechmann I, Tomkins O, Heinemann U, Friedman A. Lasting blood-brain barrier disruption induces epileptic focus in the rat somatosensory cortex. J Neurosci 2004;24:7829–7836. [PubMed: 15356194]

Sisodiya SM, Martinian L, Scheffer GL, Van DV, Scheper RJ, Harding BN, Thom M. Vascular colocalization of P-glycoprotein, multidrug-resistance associated protein 1, breast cancer resistance protein and major vault protein in human epileptogenic pathologies. Neuropathol Appl Neurobiol 2006;32:51–63. [PubMed: 16409553]

Sokol DK, Demyer WE, Edwards-Brown M, Sanders S, Garg B. From swelling to sclerosis: acute change in mesial hippocampus after prolonged febrile seizure. Seizure 2003;12:237–240. [PubMed: 12763472]

Stolp HB, Dziegielewska KM, Ek CJ, Habgood MD, Lane MA, Potter AM, Saunders NR. Breakdown of the blood-brain barrier to proteins in white matter of the developing brain following systemic inflammation. Cell Tissue Res 2005a;320:369–378. [PubMed: 15846513]

Stolp HB, Dziegielewska KM, Ek CJ, Potter AM, Saunders NR. Long-term changes in blood-brain barrier permeability and white matter following prolonged systemic inflammation in early development in the rat. Eur J Neurosci 2005b;22:2805–2816. [PubMed: 16324115]

Tomkins O, Shelef I, Kaizerman I, Eliushin A, Afawi Z, Misk A, Gidon M, Cohen A, Zumsteg D, Friedman A. Blood-brain barrier disruption in post-traumatic epilepsy. J Neurol Neurosurg Psychiatry 2008;79:774–777. [PubMed: 17991703]

Uva L, Librizzi L, Marchi N, Noe F, Bongiovanni R, Vezzani A, Janigro D, de Curtis M. Acute induction of epileptiform discharges by pilocarpine in the in vitro isolated guinea-pig brain requires enhancement of blood-brain barrier permeability. Neuroscience 2008;151:303–312. [PubMed: 18082973]

van Vliet EA, da Costa AS, Redeker S, van Schaik R, Aronica E, Gorter JA. Blood-brain barrier leakage may lead to progression of temporal lobe epilepsy. Brain 2007;130:521–534. [PubMed: 17124188]

Vernino S. Autoimmune and paraneoplastic channelopathies. Neurotherapeutics 2007;4:305–314. [PubMed: 17395141]

Vincent A, Roberts M, Willison H, Lang B, Newsom-Davis J. Autoantibodies, neurotoxins and the nervous system. J Physiol Paris 1995;89:129–136. [PubMed: 7581302]

Wieshmann UC, Woermann FG, Lemieux L, Free SL, Bartlett PA, Smith SJ, Duncan JS, Stevens JM, Shorvon SD. Development of hippocampal atrophy: a serial magnetic resonance imaging study in a patient who developed epilepsy after generalized status epilepticus. Epilepsia 1997;38:1238–1241. [PubMed: 9579926]

Wolman M, Klatzo I, Chui E, Wilmes F, Nishimoto K, Fujiwara K, Spatz M. Evaluation of the dye-protein tracers in pathophysiology of the blood-brain barrier. Acta Neuropathol 1981;54:55–61. [PubMed: 7234328]

Yarowsky PJ, Krueger BK. Development of saxitoxin-sensitive and insensitive sodium channels in cultured neonatal rat astrocytes. J Neurosci 1989;9:1055–1061. [PubMed: 2538579]

Zhou S, Chan E, Duan W, Huang M, Chen YZ. Drug bioactivation, covalent binding to target proteins and toxicity relevance. Drug Metab Rev 2005;37:41–213. [PubMed: 15747500]

Ziylan YZ, Robinson PJ, Rapoport SI. Blood-brain barrier permeability to sucrose and dextran after osmotic opening. Am J Physiol 1984;247:R634–R638. [PubMed: 6208789]

Zylber-Katz E, Gomori JM, Schwartz A, Lossos A, Bokstein F, Siegal T. Pharmacokinetics of methotrexate in cerebrospinal fluid and serum after osmotic blood-brain barrier disruption in patients with brain lymphoma. Clin Pharmacol Ther 2000;67:631–641. [PubMed: 10872645]

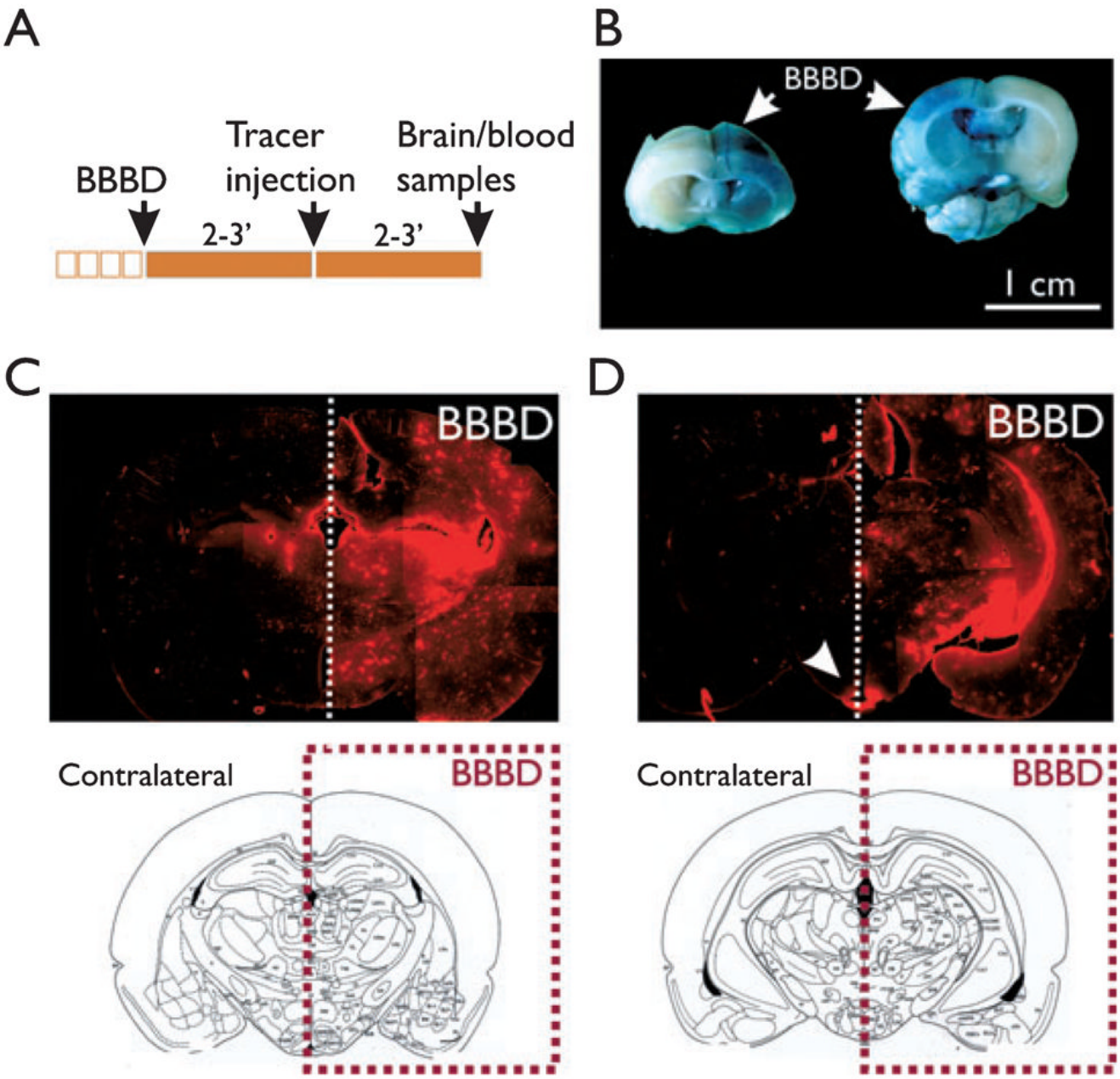


**Figure 1.**

Effect of blood–brain barrier disruption (BBBD) on serum protein extravasation. (**A**) Time line to describe the intervals between various procedures. (**B**) Gross anatomic analysis of Evans Blue leakage across the BBB. Note the pronounced extravasation of dye and the hemispheric specificity of the BBBD procedure. (**C, D**) Micrographs describing the effect of intraarterial mannitol on Evans Blue (seen in red under UV light). Note the patchy extravasation profile of Evans Blue in both gray and white matter. The diagrams show the anatomic level of the micrographs. The images in **C** and **D** were obtained at approximately −2.14 and −4.5 mm from bregma (Stolp et al., 2005a). The arrow in **D** points to a bilateral leakage in hypothalamic regions devoid of BBB protection (see also Cavaglia et al., 2001).

*Epilepsia* © ILAE

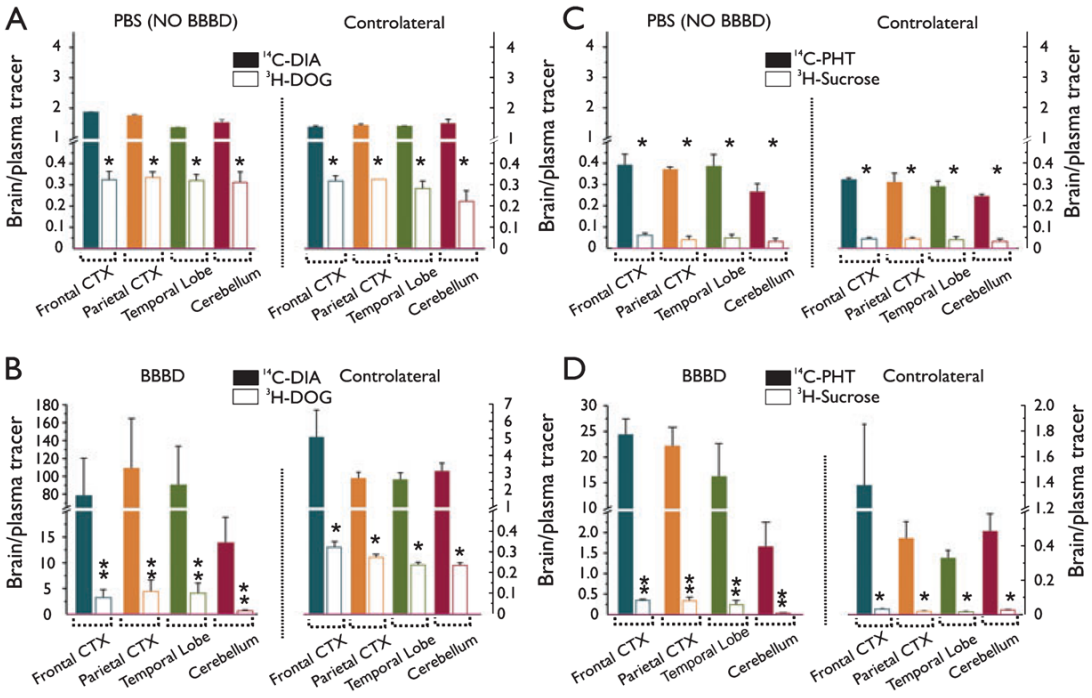


**Figure 2.**

Blood–brain barrier disruption (BBBD) causes profound changes in drug distribution in the central nervous system (CNS). (**A, C**) Control experiments (5 animals per group) demonstrate that the procedure of intraarterial catheterization and drug delivery does not affect the integrity of the BBB. Saline injection did not affect the transendothelial delivery of the tracers. (**B**) BBBD caused a large increase of radiolabeled diazepam and deoxy-glucose (DOG) (n = 5) in the CNS (note the different scale in the two panels in (**B**). (**D**) CNS drug levels depend on the lipophilicity of the drug. Therefore, even within the narrow range of log P, phenytoin accumulated less in the CNS than its slightly more lipophilic counterpart, diazepam (n = 5). Sucrose and DOG were used as hydrophilic tracers for these experiments. The internal control consisted of the undisrupted hemisphere. Note that the contralateral hemisphere was unaffected by intraarterial mannitol osmotic effects on BBB endothelial cells. The asterisks refers to $p < 0.05$; the double asterisk refers to $p < 0.01$.

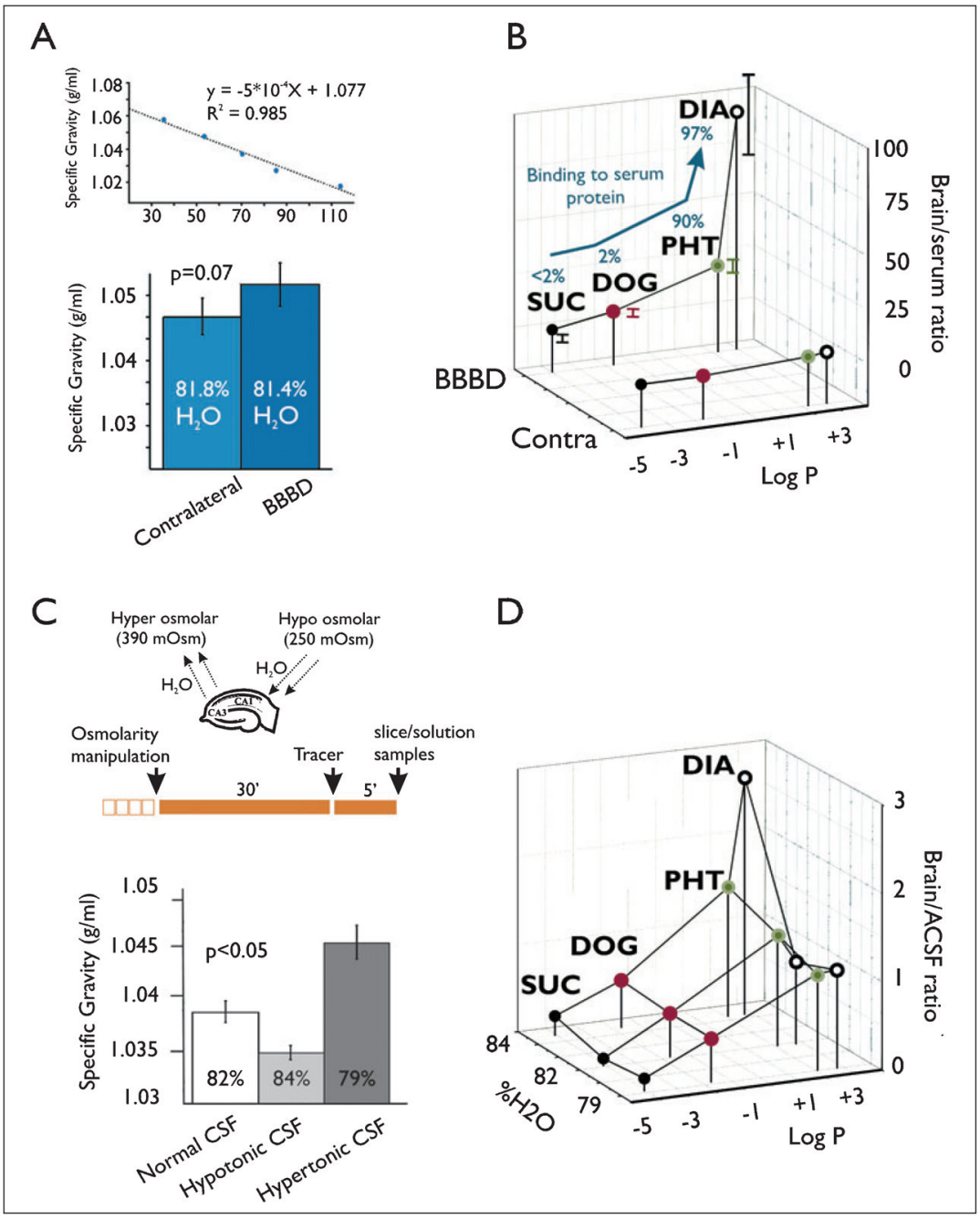


**Figure 3.**

Lack of significant effect of blood–brain barrier disruption (BBBD) on brain water content and modest effect of parenchymal edema on drug uptake. (**A**) Calibration curve for the determination of water content and determination of water brain content after BBBD (n = 5 rats). Please see Methods for experimental details. (**B**) Modest effect of BBBD on brain water content and effects of BBBD on penetration of drugs in vivo. The extent of protein binding to the drug is reported as a label in *blue*. A similar experimental approach was then used in vitro (shown in **C**), where water content was osmotically controlled as described in the Methods (five slices per experimental condition from five rats, tot = 15). (**D**) Note that manipulation of water content in vitro had only a modest effect on drug diffusion into brain tissue, suggesting

that parenchymal water content is not per se sufficient to drastically alter drug pharmacokinetic properties (5 slices per experimental condition, for a total of 30 slices). The effect of BBBD on brain water content in vivo, as evaluated 2–3 min after osmotic opening, was minimal; yet the effect of the procedure was significantly larger than that observed in vitro (note the different scale in the two tridimensional plots).
*Epilepsia* © ILAE

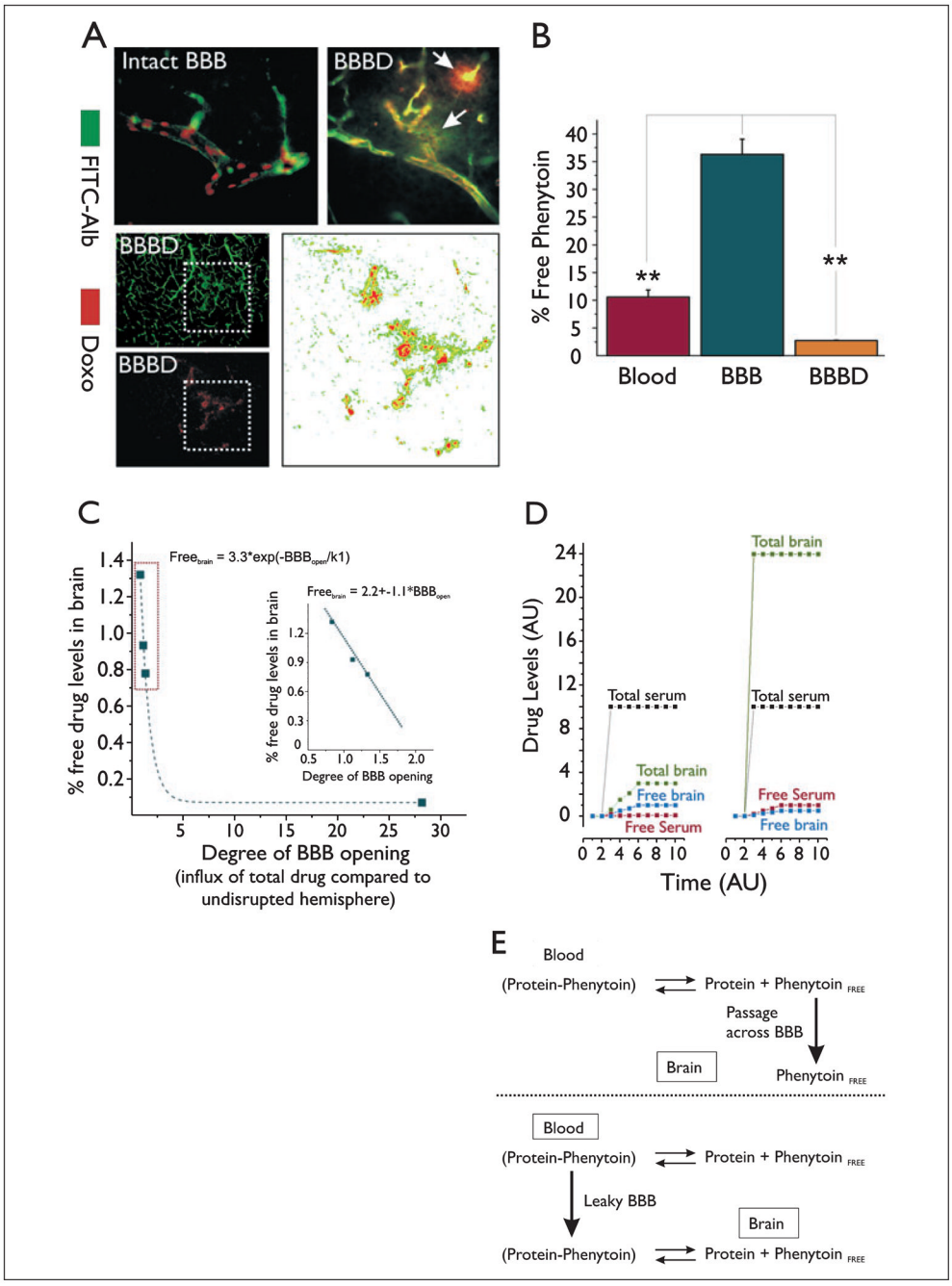


**Figure 4.**

Effect of blood–brain barrier (BBB) osmotic disruption on serum protein and drug influx into the brain. (**A**) Hemispheric disruption promotes widespread leakage of serum albumin. Visualization of protein [fluorescein isothiocyanate (FITC)–albumin, in *green*) and doxorubicin (DOXO, in *red*) extravasation in regions of intact or leaky BBB reveal regional overlap between DOXO and FITC-albumin. Note that intravascular protein and drug fail to migrate across an intact BBB (upper panel), whereas protein and drugs extravasate in the same location when the BBB is breached. The images depicted are relative to the temporal cortex. This is because of the tight binding of serum protein to lipophilic drugs. The merged image shows the overlap of green and red fluorescence after background subtraction. The

consequences of BBB disruption (BBBD) were also quantified for an antiepileptic drug [phenytoin (**B**)]. Note that the free drug levels in the brain were greatly reduced by osmotic BBBD and subsequent protein extravasation. (**C**) Relationship between extent of total drug extravasation and free levels of phenytoin on the brain. The data were obtained by comparing free and total drug levels in disrupted or undisrupted hemispheres (n = 4 rats). The whole spectrum of BBBD was fitted by an exponential. The *dashed box* highlights the data points shown in the *insert*, where data points were fitted by a least squares routine. Each data point was taken from an individual experiment. Both graphs demonstrate an inverse relationship between BBBD and free phenytoin levels, regardless of the extent of BBBD achieved. A schematic representation of the data is shown in (**D**); see text for details. The equations in (**E**) were used as a model for the plot in **D**. AU, arbitrary units. Free and bound values for phenytoin were taken from the data in (**B**) and (**C**).
*Epilepsia* © ILAE

**Table 1**

Physical–chemical and biologic properties of molecules and drugs used for this study

| Compound | MW | Log P (octanol/$H_2O$) | Protein binding (%) | %Free (serum) | Permeability coeff. (across BBB, $10^{-6}$ cm/s) |
|---|---|---|---|---|---|
| Phenytoin | 252.3 | 2.47 (Leveugle et al., 1998) | 90 | 8–14 | 26.7 (Dehouck et al., 1997) |
| Deoxy-glucose | 164.2 | −2.97 (Neuberger et al., 1992) | 2 | >98 | <1.0 (Mielke et al., 1997) |
| Sucrose | 342.3 | −3.61 (Neuberger et al., 1992) | <2 | >98 | 6.0 (Schubart et al., 2000) |
| Doxorubicin | 543.5 | 0.60 (Yarowsky & Krueger, 1989) | 71 | ~30 | 4.5 (Nishino et al., 1997) |
| Diazepam | 284.7 | 2.80 | 97 | 1.25 | 33.4 (Dehouck et al., 1997) |
| FITC-Albumin | ~66,400 | N/A | >98 | <2 | Very low |
| Evans Blue-Albumin | ~67,000 | N/A | >98 | <2 | Very low |

MW, molecular weight.